Materials Science and Engineering A 528 (2011) 1828–1832

Contents lists available at ScienceDirect

Materials Science and Engineering A

journal homepage: www.elsevier.com/locate/msea

Microstructural stability of Cu processed by different routes of severe plastic deformation

J. Gubicza[a,*], S.V. Dobatkin[b], E. Khosravi[a], A.A. Kuznetsov[b], J.L. Lábár[a,c]

[a] Department of Materials Physics, Eötvös Loránd University, Pázmány Péter s. 1/A, H-1117 Budapest, Hungary
[b] A.A. Baikov Institute of Metallurgy and Materials Science, Russian Academy of Sciences, Moscow, Russia
[c] Research Institute for Technical Physics and Materials Science, P.O.Box 49, H-1525 Budapest, Hungary

ARTICLE INFO

Article history:
Received 17 June 2010
Received in revised form 9 November 2010
Accepted 9 November 2010

Keywords:
Nanostructured materials
Equal channel angular processing
High-pressure torsion
Dislocations
Aging

ABSTRACT

The thermal stability of ultrafine-grained (UFG) microstructure in Cu processed by different routes of severe plastic deformation (SPD) was studied at both high and room temperatures (RT). It was found that the microstructures produced by multi-directional forging or twist extrusion were more stable than those obtained by equal-channel angular pressing (ECAP) or high-pressure torsion (HPT). During storage of the ECAP-processed specimen at RT for 4 years the vacancy concentration reduced significantly while the dislocation density and the crystallite size remained unchanged. In the case of the HPT-processed sample both grain-growth and reduction of the dislocation density were observed.

1. Introduction

Severe plastic deformation (SPD) procedures are attractive methods for producing bulk ultrafine-grained (UFG) metals [1]. In the last decades, several methods such as equal-channel angular pressing (ECAP), high-pressure torsion (HPT), multi-directional forging (MDF) and twist extrusion (TE) were developed for introducing severe plastic deformation into metals and alloys [2]. These procedures are quite different both in the physical principle of their operations and in the sizes of the workable pieces. Because of their practical importance, UFG face centered cubic (fcc) metals processed by different SPD procedures have been studied extensively (e.g. in Ref. [3]). The evolution of the microstructure as a function of strain, the characteristic parameters of microstructure in the saturation state and the correlation between the microstructure and the mechanical behavior have been established in detail. The thermal stability of the UFG microstructure processed by SPD is of great importance from the point of view of practical applications of these materials. Thus, if the fine grains become coarsened during their service life-time, their unique properties including their high strength will be lost. The stability of fcc metals processed by ECAP and HPT has been investigated by differential scanning calorimetry [4]. It was found that the higher the imposed strain, the lower the onset temperature of recovery/recrystallization of the UFG microstructure [5]. Previous studies [6–11] have also shown that the UFG microstructure in Cu and Ag samples processed by ECAP at room temperature (RT) partially recovered and/or recrystallized during storage at the temperature of processing. The aim of the present study is to investigate the effect of the applied SPD method on the thermal stability of UFG Cu processed at RT. Samples produced by MDF, TE, ECAP and HPT methods are compared by their microstructural stability at room and high temperatures. It should be noted that the applied SPD methods differ in many points, e.g. in the applied stress tensor, the character of the processing monotonicity, strain rate, etc. In spite of this fact, we did not force to carry out the different SPD procedures in the same conditions (e.g. at same strain rates) since our goal was to study the difference in stability of samples processed by similar ways as usually applied in the literature.

2. Experimental materials and procedures

Oxygen-free copper (99.98%) samples were processed by 15 passes of TE, 20 cycles of MDF, 25 passes of ECAP and 25 revolutions of HPT at RT. In the TE procedure, the billet had a cross-section of 18 mm × 28 mm and a length of 80 mm. The extrusion die has a twist angle of $\beta = 53^\circ$. In this configuration, 15 passes of TE corresponds to a strain of about 14 [12]. The MDF process was carried out on a rod having an initial diameter of 40 mm and length of 70 mm. 20 cycles of MDF corresponds to an equivalent strain of

* Corresponding author. Tel.: +36 1 372 2876; fax: +36 1 372 2811.
E-mail address: gubicza@metal.elte.hu (J. Gubicza).

0921-5093/$ – see front matter © 2010 Elsevier B.V. All rights reserved.
doi:10.1016/j.msea.2010.11.026

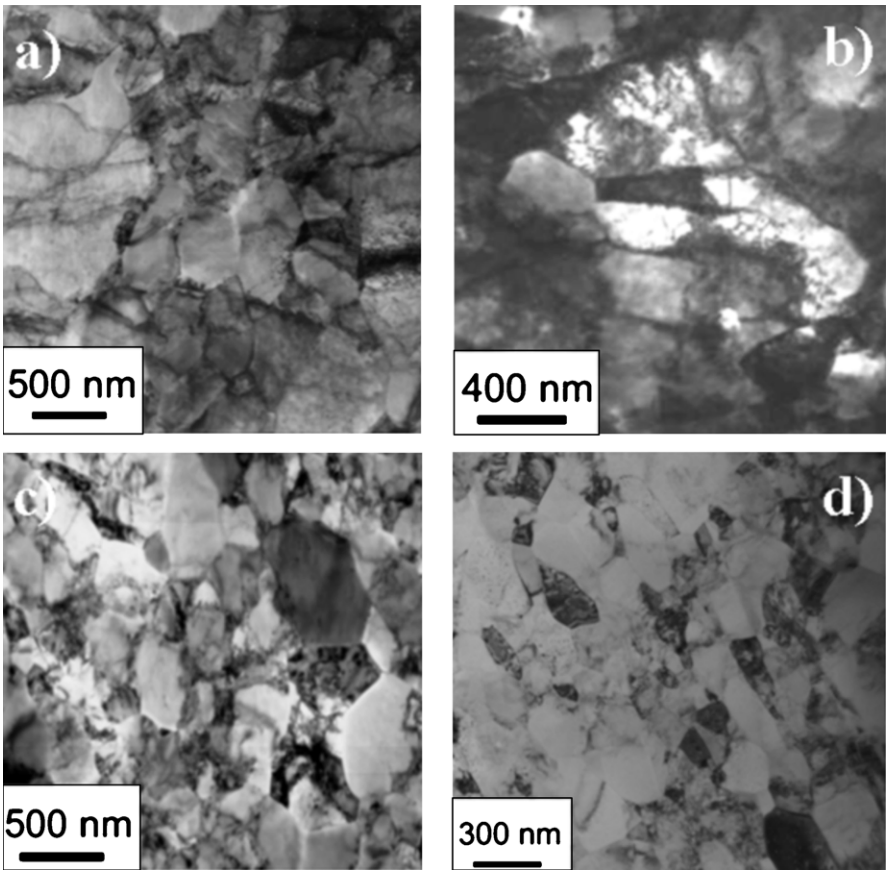

Fig. 1. TEM images showing the microstructure of Cu specimens immediately after 20 cycles of MDF (a), 15 passes of TE (b), 25 passes of ECAP (c) and 25 revolutions of HPT (d).

about 50 [13]. A sample having 20 mm in diameter and 80 mm in length was processed for 25 passes of ECAP following route B_C. The ECAP die has an internal channel angle of 90° and an outer arc of curvature of 0° at the intersection of the two parts of the channel. In this configuration, 25 passes correspond to an equivalent strain of ~29 [14]. The HPT processing was carried out on a disk having 10 mm in diameter and 0.6 mm in initial thickness. After 25 revolutions, the thickness was reduced to 0.2 mm. The applied pressure was 4 GPa during HPT. The HPT-processed disk was studied at the half-radius where the equivalent strain was about 567 assuming a mean thickness of 0.4 mm [15]. The hardness of the SPD-processed Cu samples was measured after annealing for 1 h at different temperatures between 293 and 623 K with an applied load of 500 mN. The thermal stability was also monitored by differential scanning calorimetry (DSC) at a heating rate of 40 K/min. For studying the stability at RT, the microstructures immediately after SPD and after storage at RT for 4 years were compared.

The microstructures of Cu samples were investigated by transmission electron microscopy (TEM) using JEM-100CX and Philips CM-20 microscopes operating at 100 and 200 kV, respectively. In the cases of TE, MDF and ECAP, the TEM images were taken on the cross-sections perpendicular to the TE direction, the longitudinal axis after the last MDF step and the axis of the output channel of the last ECAP pass, respectively. For the HPT-processed sample, the TEM foil was prepared at the half-radius of the disk. The microstructures were also investigated by X-ray diffraction line profile analysis. The X-ray line profiles were measured by a special high-resolution diffractometer (Nonius FR591) using Cu $K\alpha_1$ radiation ($\lambda = 0.15406$ nm). The line profiles were evaluated by the convolutional multiple whole profile (CMWP) fitting procedure described elsewhere [16]. This method gives the crystallite size, the dislocation density and the twin boundary frequency with good statistics, where the twin boundary frequency is defined as the relative fraction of the twin boundaries among {1 1 1} planes along their normal vector.

3. Results and discussion

3.1. High temperature thermal stability of microstructures processed by different SPD methods

TEM images of the microstructures of Cu samples processed by MDF, TE, ECAP and HPT methods are shown in Fig. 1. In the TEM images the majority of grains are equiaxed, only a few slightly elongated grains can be observed. The average grain size determined by TEM for Cu samples is listed in Table 1. All the grain size values are slightly above 200 nm, except for the HPT-processed specimen having a grain size of about 160 nm. According to the literature data, these values are around the minimum grain size that can be achieved in bulk Cu by SPD at RT. The crystallite size, the dislocation

Table 1
The average grain size (D_{TEM}) determined by TEM, the area-weighted mean crystallite size ($\langle x \rangle_{area}$), the dislocation density (ρ) and the twin frequency (β) obtained from X-ray line profile analysis and the onset temperature of recovery/recrystallization (T_{onset}) measured by DSC at a heating rate of 40 K/min for Cu processed by different SPD methods.

	D_{TEM} [nm]	$\langle x \rangle_{area}$ [nm]	ρ [10^{14} m^{-2}]	β [%]	T_{onset} [K]
20 MDF	225	142 ± 15	7 ± 1	0.0 ± 0.1	581 ± 3
15 TE	225	107 ± 12	10 ± 1	0.0 ± 0.1	572 ± 3
25 ECAP	215	101 ± 15	15 ± 1	0.1 ± 0.1	469 ± 2
25 HPT	160	75 ± 9	37 ± 4	0.1 ± 0.1	419 ± 2

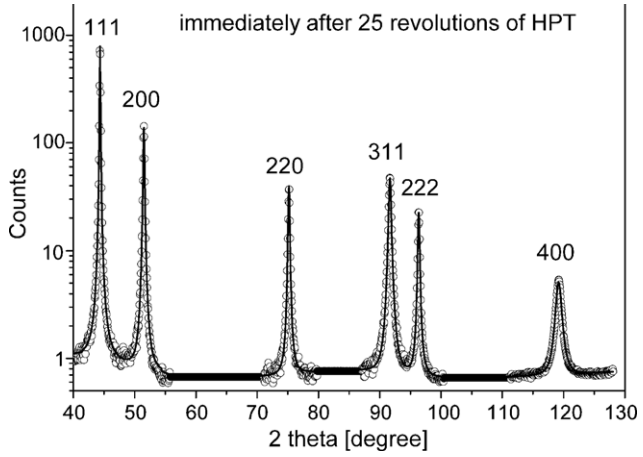

Fig. 2. CMWP fitting of the X-ray diffraction pattern measured immediately after 25 revolutions of HPT. Open circles and solid line represent the measured and the fitted patterns, respectively. The intensity is in logarithmic scale.

density and the twin boundary frequency were determined by X-ray line profile analysis. As an example, Fig. 2 illustrates the CMWP fitting of the X-ray diffraction pattern measured immediately after 25 revolutions of HPT. Open circles and solid line represent the measured and the fitted patterns, respectively. The parameters of the microstructure obtained by X-ray line profile analysis are listed in Table 1. The lowest dislocation densities were measured after MDF and TE processes while the largest value was obtained after HPT. The higher the dislocation density, the smaller the crystallite size for the four studied samples. The twin boundary frequency for all samples was relatively low ($0.1 \pm 0.1\%$), close to the detection limit of this quantity for the applied experimental setup of X-ray line profile analysis. The extremely high dislocation density ($37 \pm 4 \times 10^{14}\,m^{-2}$) after HPT is in good agreement with the values obtained by other authors [11].

The very high dislocation density after HPT can be attributed to the high pressure ($p = 4$ GPa) applied during HPT that may affect the climb-controlled annihilation of dislocations in the following ways:

i) The climb velocity is proportional to the diffusion coefficient [17] that depends on the concentration and the migration enthalpy of vacancies. Previous experiments have shown that in SPD-processed metals a large amount of vacancies are formed due to forced plasticity, therefore their concentration is much higher than the equilibrium value [18–25]. When a high pressure is applied in SPD-processing, larger work (by pV_v where V_v is the volume of a vacancy) is needed for vacancy formation but this does not reduce the vacancy concentration as the necessary extra work is supplied by the external forces. Rather an increased vacancy concentration was observed in previous studies [18,20–22] with increasing the pressure of HPT that can be explained by the suppressed vacancy annihilation at dislocations due to their slower migration. The reduction of vacancy migration at higher pressure is caused by the increase of the migration enthalpy by pV_v. The increased difficulty of vacancy migration due to the high pressure applied during HPT hinders effectively the annihilation of dislocations by climb compared to other SPD-processing.
ii) In fcc metals the climb velocity of dissociated dislocations is inversely proportional to the square of splitting distance between Shockley partials [17]. The value of equilibrium splitting distance between partials for edge dislocations in Cu is about 2.3 nm [10]. The very large loading on the anvils during HPT most probably results not only in a high hydrostatic pressure but also in high shear stresses since the idealized constrained conditions are usually not achieved. The shear stresses acting on the slip plane of a dislocation perpendicular to the Burgers-vector can decrease or increase the splitting distance by pushing the partials towards each other or pulling the partials in opposite directions, respectively, depending on the stress orientation. Therefore, the higher shear stresses during HPT may result in much larger or smaller splitting distance depending on their directions. As the splitting distance without stresses is not very large in Cu due to the medium value of its stacking fault energy (data between 45 and 78 mJ/m^2 are reported in the literature [26,27]), therefore the stresses pushing the partials towards each other do not accelerate climb very much. At the same time, the high stresses resulting in much larger splitting distance slow down climb effectively. Due to the effects of (i) and (ii), the high pressure applied during HPT retard climbing process of annihilation of dislocations thereby increasing the dislocation density in the HPT-processed Cu sample.

The high stresses have also an effect on the cross-slip of dislocations. For screw dislocations the splitting distance between partials (~0.9 nm [10]) is smaller than for edge dislocations, therefore cross-slip occurs relatively easily even without stresses. The cross-slip process is also very sensitive on stresses because shear stresses pushing the partials towards each other in the initial glide plane or shear stresses pulling the partials in opposite directions in the cross-slip plane assist the cross-slip process effectively [28]. At the same time, stresses increasing the distance between partials in the initial glide plane or reducing this distance in the cross-slip plane hinder the cross-slip of screw dislocations. During HPT processing, the high applied loading most probably increases the stresses which can assist or hinder the cross-slip of screw dislocations depending on the stress orientation. Due to the not very large degree of dislocation dissociation in Cu, the increased assisting stresses have only a minor promotion effect on cross-slip. At the same time, the high hindering stresses can increase effectively the degree of dislocation dissociation resulting in a difficult cross-slip and therefore an obstruction of annihilation of screw dislocations during HPT which also contributes to the very high dislocation density. The above considerations suggests that both climb and cross-slip of dislocations were retarded due to the high load applied during HPT that explains the extremely high dislocation density measured immediately after HPT-processing. Our argumentation is also supported by previous observations on increasing dislocation density with increasing pressure applied during HPT [e.g. 18,24].

During annealing of the SPD-processed samples in DSC an exothermic peak evolved which corresponds to the recovery and recrystallization of the microstructure as was shown in previous studies (e.g. in Ref. [4]). Table 1 reveals that despite the similar grain size values of the samples processed by various SPD methods, the onset temperatures of recovery/recrystallization are very different. It can be established that the higher the dislocation density and lower the crystallite size, the lower the onset temperature of recovery/recrystallization, i.e. the samples produced by MDF and TE show the highest thermal stability while the HPT-processed specimen has the lowest stability. This result is also supported by the change of hardness as a function of annealing temperature presented in Fig. 3. The hardness of the sample processed by HPT starts to decrease at the lowest temperature compared to other specimens while the hardness of the MDF and TE samples remains unchanged up to relatively high temperatures. It is noted that the very high dislocation density after HPT is most probably accompanied by very large long-range internal stresses. These stresses may assist annihilation of dislocations thereby resulting in lower temperature of recovery/recrystallization as it has been already suggested in previous papers [e.g. 24]. It is also noted that beside

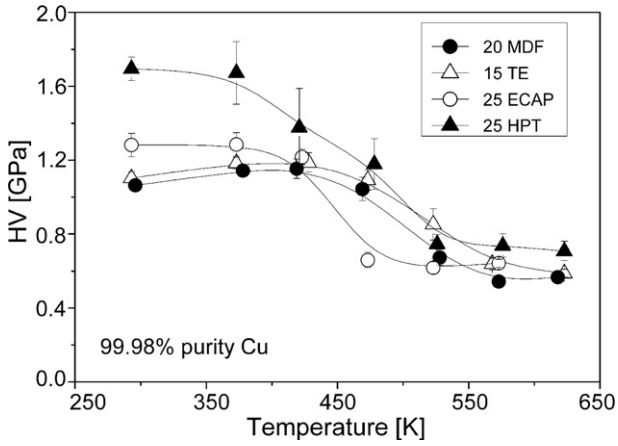

Fig. 3. The hardness as a function of annealing temperature for Cu samples processed by 20 cycles of MDF, 15 passes of TE, 25 passes of ECAP and 25 revolutions of HPT.

the grain size and the dislocation density other features of the microstructure (e.g. grain boundary character) may also influence the stability of the SPD-processed samples. Electron backscatter diffraction (EBSD) analysis (not shown here) revealed that the fraction of high angle grain boundaries has similar high values (80–94%) for all the studied samples, therefore most probably it does not increase significantly the difference in stability. In the cases of the less stable ECAP and HPT samples, the stability of the SPD-processed microstructures were studied during storage of the samples at RT for 4 years as presented in the next section.

3.2. Stability of the Cu samples processed by ECAP and HPT during storage at room temperature

In a recently published paper [25] the parameters of the severely deformed microstructure in the ECAP-processed sample were determined both immediately after 25 passes and storage for 4 years at RT. All parameters of the microstructure determinable by X-ray line profile analysis (crystallite size, dislocation density, edge/screw character and arrangement of dislocations and twin boundary frequency) remained unchanged within the experimental error during 4 years of storage. At the same time, the stored energy measured by DSC at 40 K/min heating rate decreased from 1.0 ± 0.1 J/g to 0.37 ± 0.04 J/g during storage for 4 years. These experimental results suggest that the reduction of the stored energy during storage can be attributed to the annihilation of such defects which cannot be evaluated by line profile analysis. These defects may be point defects such as vacancies or vacancy agglomerates which form in a high concentration during severe plastic deformation as shown in previous papers [18–25]. Assuming that the reduction of the stored energy is attributed solely to the loss of vacancies, the decrease of vacancy concentration during the storage for 4 years was determined from the change of stored energy using Eq. (1) in Ref. [25]. The change of vacancy concentration was 3.4×10^{-4} that is a similar value as the vacancy content determined previously for Cu samples immediately after ECAP by electrical resistivity measurement or a combination of X-ray line profile analysis and calorimetry [19]. Therefore, most probably the majority of vacancies formed during ECAP disappeared during storage for 4 years at RT. It is worth to note that the reduction of vacancy concentration was not accompanied by the annihilation of dislocations as it was shown by X-ray line profile analysis. The very large excess of vacancies may decrease by migration along the boundaries of UFG grains to the free surface of the samples and/or by annealing at small dislocation loops having a dimension of several nanometers that results in the annihilation of these loops. These loops are invisible by X-ray line profile analysis due to their strongly shielded strain field and small dimensions.

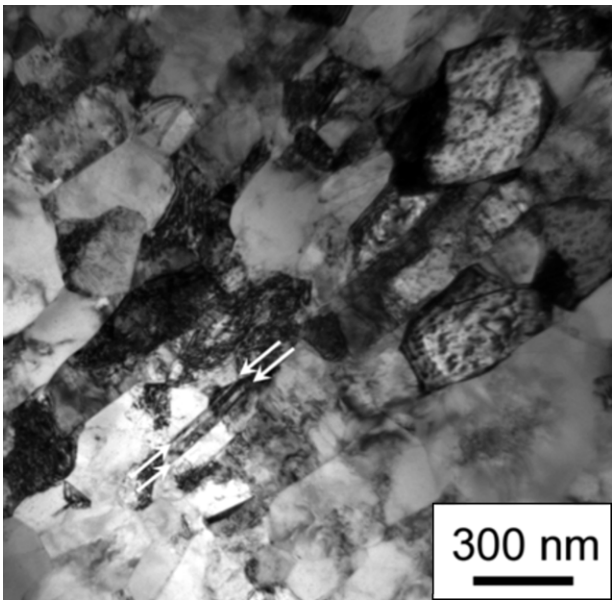

Fig. 4. TEM image taken on the HPT-processed sample after storage at room temperature for 4 years.

The stability of the least stable HPT-processed sample was also studied during storage at RT for 4 years. Fig. 4 shows a TEM image taken for the HPT-processed Cu sample after 4 years of storage. The comparison of this image with that obtained immediately after HPT (see Fig. 1d) revealed a growth of the mean grain size from about 160 nm to 250 nm. It is noted that some relatively large grains with the size of about 600 nm were also observed after storage for 4 years. X-ray line profile analysis showed that the average crystallite size increased from 75 ± 9 to 122 ± 15 nm while the dislocation density decreased from $37 \pm 4 \times 10^{14}$ to $13 \pm 2 \times 10^{14}$ m^{-2} during storage for 4 years. Simultaneously, the twin boundary frequency increased from $0.1 \pm 0.1\%$ to $0.3 \pm 0.1\%$. In the TEM image of Fig. 4 some twin boundaries are indicated by white arrows. These changes of the microstructure characteristics indicate recovery and/or recrystallization during storage of the sample. As it was discussed above, the high pressure applied during HPT hindered the annihilation processes of dislocations resulting in very high dislocation density and small grain size. During storage of the sample, this extremely high dislocation density and the very small grain size are the driving force of the microstructure transformation. The high density of dislocations results in large internal stresses. Therefore, when the pressure was released after HPT, the vacancy diffusion became faster resulting in annihilation of edge dislocations by climb. Moreover, the internal stresses most probably also cause cross-slip of dissociated screw dislocations having high density after HPT. The dislocation density can also decrease by twinning at dislocation pile-ups developed at glide obstacles. If the local stresses at these obstacles exceed the critical stress required for twin nucleation, after an incubation time twins are formed at the expense of dislocations in the pile-ups [29]. The operation of this mechanism is supported by the increase of twin boundary frequency from $0.1 \pm 0.1\%$ to $0.3 \pm 0.1\%$ during storage. It is noted, however, that partial recrystallization may also contribute to the higher twin boundary frequency as twinning usually occurs during recrystallization of fcc metals.

The large reduction of vacancy concentration did not yield significant change of the hardness (1.28 GPa) for the ECAP-processed

sample during storage for 4 years. At the same time, the hardness of the HPT-processed sample decreased from 1.69 ± 0.06 GPa to 1.07 ± 0.12 GPa during storage for 4 years as a result of recovery/recrystallization of the microstructure. It should be noted that we have already reported similar self-annealing in ECAP-processed Ag. Then we argued that the delayed recovery of the severely deformed microstructure was caused by the high degree of dislocation dissociation due to the very low stacking fault energy of Ag (data between 16 and 22 mJ/m^2 are reported in the literature [26,27]) and this phenomenon most probably could not occur in Cu having medium value of stacking fault energy. The present results are not in contradiction with this statement as the very large pressure during HPT also yielded a high degree of dislocation dissociation in some volumes of the Cu sample thereby resulting in a delayed recovery during storage. As in this report the microstructure and the hardness were examined only immediately after HPT and 4 years later, further studies are planned to reveal their evolutions as a function of storing time.

4. Summary

The thermal stability of Cu samples processed by 15 passes of TE, 20 cycles of MDF, 25 passes of ECAP and 25 revolutions of HPT at RT was investigated at room and high temperatures. The following conclusions can be drawn from our experimental results:

1. Despite the similar grain sizes (about 200 nm), the Cu samples deformed by various SPD methods showed different thermal stability at high temperatures. It was found that the thermal stability decreased in the order of MDF, TE, ECAP and HPT which correlates to the increase of dislocation density and the decrease of the crystallite size.
2. During storage of the sample processed by ECAP at RT for 4 years, the excess vacancy concentration was reduced by 3.4×10^{-4} while the crystallite size and the dislocation structure remained unchanged. In the case of the HPT-processed sample, the grain size and the twin boundary frequency increased while the dislocation density decreased during storage at RT for 4 years. This recovery and/or recrystallization after HPT are caused by the extremely high dislocation density and small grain size that can be attributed to the retarded annihilation of dislocations during HPT-processing due to the high applied pressure.

Acknowledgements

This work was supported in part by the Hungarian Scientific Research Fund, OTKA, Grant No. K-81360. The European Union and the European Social Fund have provided financial support to this project under grant agreement no. TÁMOP 4.2.1./B-09/1/KMR-2010-0003.

References

[1] R.Z. Valiev, R.K. Islamgaliev, I.V. Alexandrov, Prog. Mater. Sci. 45 (2000) 103–189.
[2] R.Z. Valiev, Y. Estrin, Z. Horita, T.G. Langdon, M. Zehetbauer, Y.T. Zhu, JOM 58 (4) (2006) 33–39.
[3] N.Q. Chinh, J. Gubicza, T.G. Langdon, J. Mater. Sci. 42 (2007) 1594–1605.
[4] N. Gao, M.J. Starink, T.G. Langdon, Mater. Sci. Technol. 25 (2009) 687–698.
[5] J. Gubicza, L. Balogh, R.J. Hellmig, Y. Estrin, T. Ungár, Mater. Sci. Eng. A 400–401 (2005) 334–338.
[6] G. Wang, S.D. Wu, L. Zuo, C. Esling, Z.G. Wang, G.Y. Li, Mater. Sci. Eng. A 346 (2003) 83–90.
[7] Y. Estrin, N.V. Isaev, S.V. Lubenets, S.V. Malykhin, A.T. Pugachov, V.V. Pustovalov, E.N. Reshetnyak, V.S. Fomenko, L.S. Fomenko, S.E. Shumilin, M. Janecek, R.J. Hellmig, Acta Mater. 54 (2006) 5581–5590.
[8] O.V. Mishin, A. Godfrey, Metall. Mater. Trans. A 39A (2008) 2923–2930.
[9] H. Matsunaga, Z. Horita, Mater. Trans. 50 (2009) 1633–1637.
[10] J. Gubicza, N.Q. Chinh, J.L. Lábár, Z. Hegedűs, T.G. Langdon, Mater. Sci. Eng. A 527 (2010) 752–760.
[11] E. Schafler, Scripta Mater. 62 (2010) 423–426.
[12] Y. Beygelzimer, D. Orlov, V. Varyukhin, in: Y.T. Zhu, T.G. Langdon, R.S. Mishra, S.L. Semiatin, M.J. Saran, T.C. Lowe (Eds.), Ultrafine Grained Materials II, TMS (The Minerals, Metals and Materials Society), 2002, pp. 297–304.
[13] G.A. Salischev, S.V. Zherebtsov, R.M. Galeyev, in: Y.T. Zhu, T.G. Langdon, R.S. Mishra, S.L. Semiatin, M.J. Saran, T.C. Lowe (Eds.), Ultrafine Grained Materials II, TMS (The Minerals, Metals and Materials Society), 2002, pp. 123–131.
[14] Y. Iwahashi, J. Wang, Z. Horita, M. Nemoto, T.G. Langdon, Scripta Mater. 35 (1996) 143–146.
[15] A.P. Zhilyaev, T.G. Langdon, Prog. Mater. Sci. 53 (2008) 893–979.
[16] L. Balogh, G. Ribárik, T. Ungár, J. Appl. Phys. 100 (2006) 023512.
[17] A.S. Argon, W.C. Moffatt, Acta Metall. 29 (1981) 293–299.
[18] M.J. Zehetbauer, H.P. Stüwe, A. Vorhauer, E. Schafler, J. Kohout, Adv. Eng. Mater. 5 (2003) 330–337.
[19] E. Schafler, G. Steiner, E. Korznikova, M. Kerber, M.J. Zehetbauer, Mater. Sci. Eng. A 410–411 (2005) 169–173.
[20] E. Korznikova, E. Schafler, G. Steiner, M. Zehetbauer, Proc. 4th Int. Symp. on Ultrafine Grained Materials 2006 TMS Annual Meeting, TMS, Warrendale, PA, 2006, pp. 97–102.
[21] M. Zehetbauer, G. Steiner, E. Schafler, A. Korznikov, E. Korznikova, Mater. Sci. Forum 503–504 (2006) 57–64.
[22] D. Setman, E. Schafler, E. Korznikova, M.J. Zehetbauer, Mater. Sci. Eng. A 493 (2008) 116–122.
[23] A.R. Kilmametov, G. Vaughan, A.R. Yavari, A. LeMoulec, W.J. Botta, R.Z. Valiev, Mater. Sci. Eng. A 503 (2009) 10–13.
[24] D. Setman, M.B. Kerber, E. Schafler, M.J. Zehetbauer, Metall. Mater. Trans. A 41 (2010) 810–815.
[25] J. Gubicza, S.V. Dobatkin, E. Khosravi, Mater. Sci. Eng. A 527 (2010) 6102–6104.
[26] J.P. Hirth, J. Lothe, Theory of Dislocations, John Wiley, New York, 1982.
[27] L.E. Murr, Interfacial Phenomena in Metals and Alloys, Addison Wesley, Reading, MA, 1975.
[28] P.B. Escaig, J. Phys. 29 (1968) 225–239.
[29] J.B. Cohen, J. Weertman, Acta Metall. 11 (1963) 996–998.